

Organic polymer solar cell using low-temperature deposited AZO/Ag/AZO transparent electrodes

ZONG-LIANG TSENG^{b*}, LUNG-CHIEN CHEN^b, YI-CHUN TSAI^a, SHENG-YUAN CHU^{a*}

^aDepartment of Electrical Engineering, National Cheng Kung University, Tainan 70101, Taiwan, R.O.C.

^bDepartment of Electro-Optical Engineering, National Taipei University of Technology, Taipei 106, Taiwan, R.O.C.

The electrical, optical, and structural properties of indium-free Al-doped ZnO (AZO)/Ag/AZO triple-layer electrodes deposited by room temperature sputtering without post treatments were investigated. The conductivity of the AZO/Ag/AZO triple-layer electrodes grown on glass substrates can be improved by the insertion of an Ag layer. The best figure of merit value (Φ_{TC}) was $39.9 \times 10^{-3} \Omega^{-1}$ for the AZO/Ag/AZO electrodes with 8 nm-thick Ag layer. Moreover, bulk heterojunction organic polymer solar cells based on the AZO/Ag/AZO triple-layer and AZO single-layer electrodes were fabricated for a comparative study. The polymer solar cells using AZO/Ag/AZO transparent electrodes exhibited higher performance than the cell using pure AZO electrodes, due to much lower sheet resistance of the electrode. This implies that indium-free AZO/Ag/AZO triple-layer electrodes are an appropriate transparent electrode for low-cost and low-temperature processing organic photovoltaics.

(Received May 1, 2016; accepted June 7, 2017)

Keywords: Multilayer, Polymer solar cell, Electrode, Transparent, TCO

1. Introduction

In recent years, Bulk heterojunction (BHJ) organic polymer solar cells (OPVs) that can be fabricated by solution processing techniques [1] are now attracting considerable interest due to their potential applications in flexibility, large-area solar cells [2] and light weight [3] at dramatically low-costs. The key role of their device structures is transparent electrodes, which are able to receive sunlight and transport carriers. Transparent conductive oxides (TCOs) have been widely used as the transparent electrodes in the OPVs, like indium tin oxide (ITO) [4].

In addition, ZnO-based transparent conducting thin films have been intensively investigated [4]-[8] due to their lower material cost, lower deposition temperature, higher stability in activated hydrogen environments, higher optical transmission, and lower resistivity characteristics compared to those of indium tin oxide (ITO) and tin oxide (SnO₂) films. However, when deposition conditions of the ZnO films are without substrate heating or post-annealing treatment, their conductivity is limited. In order to solve this problem to improve the properties of transparent conductors, the combination of an oxide electrode and a metal, such as TCO/metal/TCO multilayer systems, has been widely studied [9]-[12]. These systems have very low sheet resistance, comparable optical transmittance in the visible range, and much lower thickness and better durability than those of single-layer TCO films. When a metal mirror layer with high reflection is embedded between two TCO layers, TCO/metal/TCO

multilayer systems can restrain the reflection from the metal in the visible region, achieving selective transparency [13]. Therefore, a thin silver (Ag) layer, the lowest resistivity of metals ($1.587 \times 10^{-6} \Omega \cdot \text{cm}$) [14], inserted between two TCO layers has been widely investigated. Various studies have shown that ITO/Ag/ITO and ZnO-based/Ag/ZnO-based multilayer electrodes have excellent electrical and optical properties [9], [15]-[18]. A comparison study of ITO/metal/ITO and ZnO/metal/ZnO was presented in 2012, which showed both multilayer structures are comparable for flexible OPVs [19]. In 2014, a flexible OPV module using ITO/metal/ITO electrode with high efficiency was reported for the first time. The important economical fact is the low amount of ITO used for the production of flexible multilayer electrode on PET [20]. However, highly conductive AZO or AZO/metal/AZO multilayer can further reduced amount of ITO as indium-free electrodes.

In the present study, we investigated a low-temperature deposited AZO/Ag/AZO (AAA) triple-layer electrodes grown on glass substrates. The excellent electrical and optical characteristics AAA multilayer electrodes were investigated and used as the transparent electrodes of the OPVs. Their device performance is discussed in the article.

2. Experimental procedure

A 30-nm-thick (bottom and top) AZO thin film was grown using a radio frequency (RF) magnetron sputtering

system with a 3-inch ZnO:Al₂O₃ ceramic target (98 wt.% ZnO: 2 wt.% Al₂O₃) at room temperature without substrate heating or post-annealing treatment. The sputtering conditions of the bottom AZO layer were as follows: a constant argon flow rate of 4 sccm, RF power of 30 W, and a working pressure of 1 mTorr. Ag layers were deposited onto the AZO film using thermal evaporation at a constant deposition rate of 0.09 nm/s. The thicknesses of AZO and Ag layers were measured using a surface profiler (Alpha-Step, KLA-Tenco). The electrical properties of the AAA structures were investigated using Hall Effect measurements (Ecopia, HMS-3000) as a function of Ag thickness, and their optical transmittances were measured by using a UV-Vis spectrophotometer (Hitachi U-3310). The structural properties of the AAA films were analyzed using the grazing incidence angle X-Ray diffraction (GIAXRD, Rigaku D/MAX2500) with CuK α radiation.

For OPVs fabrication, ZnO electron transporting layers were used a sol-gel method. monoethanolamine (MEA) and zinc acetate [Zn(CH₃COO)₂] with molar ratio of 1:1 were added to 2-Ethoxyethanol (2-MOE), followed by stirring for 24 h to achieve the sol-gel ZnO precursor solution (0.5M), Which was spin-coated at 5000 rpm for 30 s on the top of AAA films and following annealing at 180 °C for 30 minutes. Subsequently, P3HT and PCBM (1:1) in dichlorobenzene solution (40 mg/ml) were spin-coated at 500 rpm 50 s and 1600 rpm 1 s. Solvent and post-thermal annealing were treated for around 20 min and 30 min. MoO₃ and Ag were deposited by thermal evaporation. Device characterization (Area = 0.1 cm²) was performed in N₂ and measured under AM1.5G illumination condition. Incident photo-to-current conversion efficiency (IPCE) was measured by QE-R3011 measurement system (Enlitech Inc., Taiwan).

3. Results and discussion

Fig. 1 shows that the structural properties of the AAA multilayer electrodes were analyzed using X-ray diffraction. The XRD patterns exhibit only one peak representing AZO in the (002) orientation in all samples, but the (111) orientation of the Ag diffraction peak ($2\theta = 38.12^\circ$) did not appear in the pattern due to the resolution limit of XRD [12]. The intensity of the pure AZO film (0 nm-thick Ag and 60 nm-thick AZO) was stronger than that of AAA triple-layer films (30 nm-thick AZO / Ag / 30 nm-thick AZO). The reason may be due to that the Ag interlayer influence the crystal growth of the top AZO layer.

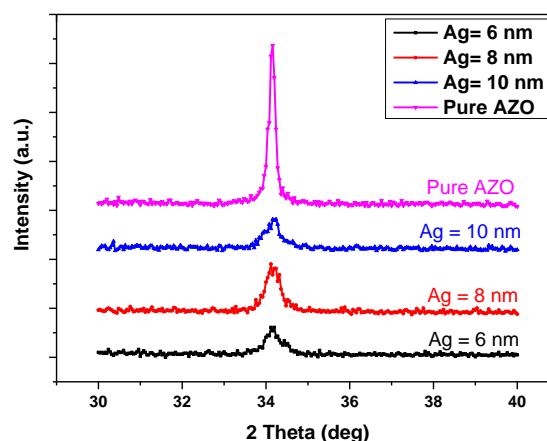


Fig. 1. XRD spectra of the AZO/Ag/AZO films deposited on glass substrates with different Ag thicknesses

Fig. 2 shows that the optical transmittance as a function of wavelength of incident light for the AAA triple-layer films grown on glass substrates. The transmittance of single-layer AZO films on glass show the best property. After an Ag layer was inserted, the optical transmittance of the AAA electrodes was significantly lower than that of single-layer AZO electrodes. Considering the optical transmittance of the AAA triple-layer structure, the AAA electrodes with the 6 nm-thick Ag layers showed low transmittance because of the light scattering by Ag islands. However, the AAA electrodes with 8-nm-thick Ag layers showed high transmittance (~89.0%), because of the surface plasmon resonance effect of the optimized Ag layer [21]. Further increasing the Ag layer thickness of 10 nm, low transmittance was obtained. This is also due to the light reflection resulted from the thicker Ag layer. The insert of Fig. 2 shows a photograph of the AAA triple-layer electrodes with 6, 8 and 10 nm-thick Ag thicknesses. The average transmittance from 400 nm to 800 nm as a function of the thickness of the Ag layer was shown in Fig. 3 (red line).

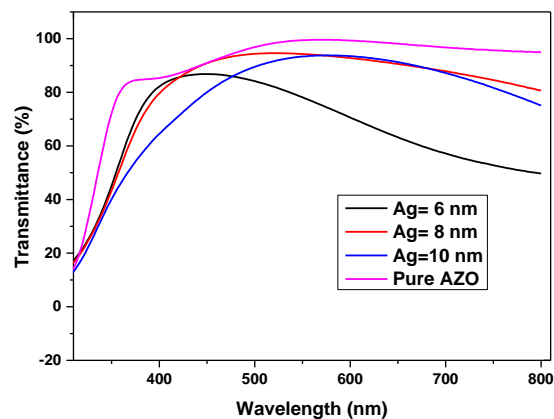


Fig. 2. Optical transmittance spectra of the AZO/Ag/AZO films deposited on glass substrates with different Ag thicknesses

Fig. 3 shows the sheet resistance (black line) of the AAA triple-layer films grown on glass substrates as a function of the thickness of the Ag layer. When the Ag thickness was gradually increased, the results of sheet resistances of both AAA structures decreased noticeably, indicating that the inserted Ag layer indeed increase the conductivity. Furthermore, when the thickness of the Ag insertion layer was over 8 nm, the decrease of the sheet resistances reached saturation due to the disconnected Ag islands transferring to continuous layer. Fahland et al. reported that a continuous layer of Ag has low absorption, high transmittance, and very good electrical conductivity [22]. In this study, it is believed that an 8-nm-thick Ag layer started to be continuous. In addition, the sheet resistance of a TCO/Ag/TCO multilayer system is mainly affected by the thickness of the Ag layer which is more important than the thickness of the top and bottom layers [23]. Actually, the top and bottom AZO layers worked in different purposes in the AAA multilayer structure. The bottom AZO layer in the AAA structures acted as a combination layer which assured a good adhesion and electrical connection between the substrate and the Ag layer, which would easily peel off if it is deposited directly on the substrate. The Ag layer mainly acted as a conductive layer, but its low transmittance limited the performance of the AAA structures. The top AZO layer in the AAA structure acted as a surface passivation layer to protect the Ag layer.

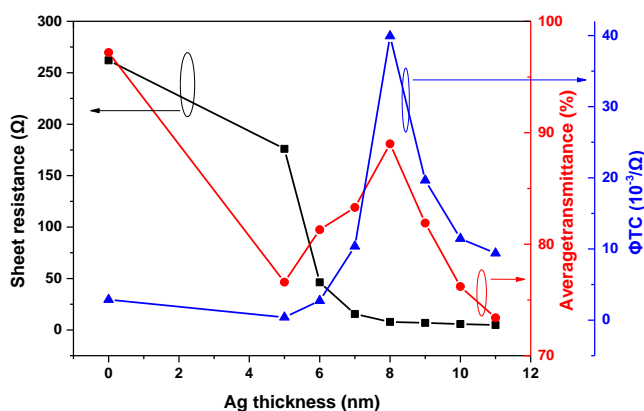


Fig. 3. Figure of merit, sheet resistance, and average transmittance at a wavelength from 400 to 800 nm for the AZO/Ag/AZO films as a function of Ag thickness

When the thickness of the Ag layer increased, the sheet resistance of the AAA multilayer electrode was improved but the optical transmittance was degenerated. Therefore, the optimization of the electrical and optical properties of Ag thin film is essential for practical applications. Haacke [24] suggested the performance of TCO films can be evaluated using the figure of merit (Φ_{TC}), which is expressed as $\Phi_{TC} = (\text{transmittance})^{10}/(\text{sheet resistance})$. Fig. 3 shows the thickness dependence of the figure of merit for the AAA multilayer electrode (blue

line). The figure of merit of the AAA films with Ag thickness of 8 nm showed the highest value of $39.9 \times 10^{-3} \Omega^{-1}$ better than that of the pure AZO films ($2.87 \times 10^{-3} \Omega^{-1}$), indicating a thin Ag layer indeed improve the electrooptical properties of the TCOs.

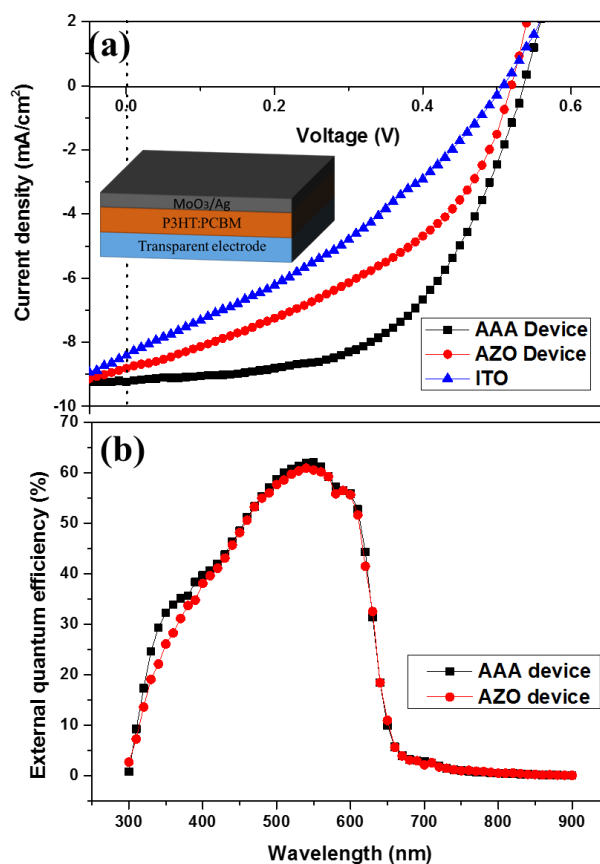


Fig. 4. (a) Current density-voltage characteristics and (b) IPCE spectra of the OPV fabricated on AAA triple-layer and AZO single-layer transparent electrodes. The insert in (a) shows a schematic of the device structure. The cell based on ITO electrode also was shown in (a)

Fig. 4 (a) shows the current density – voltage (J-V) curves of OPVs using pure AZO and AAA films (Ag = 8 nm) as transparent electrodes. The cell with AAA electrodes shows the short circuit current density (J_{sc}), the open voltage (V_{oc}), and fill factor (FF) of $9.23 \text{ mA} \cdot \text{cm}^{-2}$, 0.54V, and 55.1 %, respectively, leading to a power conversion efficiency (PCE) of 2.73 %. The OPV device using pure AZO transparent electrodes (60 nm) shows a PCE of 1.93 %, with a J_{sc} of $8.81 \text{ mA} \cdot \text{cm}^{-2}$, a V_{oc} of 0.52 V, and a FF of 42.1 %. However, the cell using ITO electrodes (sheet resistance = 10 Ω) exhibited a poor FF. It is due to the high work function of ITO electrodes in the inverted OPV device structure, resulting in inefficient exciton extraction. [25-26] The AZO and AAA electrodes show more suitable characteristics for the inverted OPV devices. Moreover, the OPV based on AAA films shows a

better Voc and FF because of their good conductivity, leading to better carrier transporting and less Voc loss. The results are consistent with the observation of the figure of merit. Fig. 4(b) show the corresponding IPCE spectra of the resulting devices of Fig. 4(a). The IPCE curve shows a strong spectral response in the range from 300 nm to 650 nm, resulted from absorption of active P3HT layers. The integrated currents (8.51 and 8.34 mA·cm⁻²) from IPCE is consistent with those obtained from the solar simulators (AM 1.5 G). Although the AAA device received fewer incident sunlight because of slightly weaker transmittance of the AAA film, higher Jsc still was obtained because of its significantly improved conductivity.

4. Conclusion

The electrical and optical characteristics of AAA triple-layer electrodes grown on glass without substrate heating or post-annealing treatment were investigated. Considering the Φ_{TC} , the AAA multilayer structure with an 8-nm-thick Ag layer exhibited optimized electrical and optical properties. Its sheet resistance values, the average optical transmittance and Φ_{TC} were 7.81 Ω , 89.0 % and 39.9 $\times 10^{-3}$ Ω^{-1} , respectively. Moreover, the OPVs based on the AAA transparent electrodes show higher power conversion efficiency than those of the OPVs prepared on the AZO single-layer electrodes due to their low sheet resistance. This indicates that the indium-free ZnO-based multilayer electrode prepared by low-temperature sputtering process is a promising material of the transparent electrode for low-cost and flexible OPVs.

Acknowledgments

This work was supported by the National Science Council of Taiwan from grants MOST 105-2218-E-027-009.

Reference

- [1] G. Li, R. Zhu, Y. Yang, *Nat. Photon.* **6**, 153 (2012).
- [2] L. Lucera, F. Machui, P. Kubis, H.-D. Schmidt, J. Adams, S. Strohm, T. Ahmad, K. Forberich, H.-J. Egelhaaf, C. J. Brabec, *Energ. Environ. Sci.* **9**, 89 (2015).
- [3] M. Kaltenbrunner, M. S. White, E. D. Głowacki, T. Sekitani, T. Someya, N. S. Sariciftci, S. Bauer, *Nat. Commun.* **3** 770 (2012).
- [4] Z. A. Wang, J. B. Chu, H. B. Zhu, Z. Sun, Y. W. Chen, S. M. Huang, *Solid State Electron.* **53**(11), 1149 (2009).
- [5] H. J. Cho, S. U. Lee, B. Hong, Y. D. Shin, J. Y. Ju, H. D. Kim, M. Park, W. S. Choi, *Thin Solid Films* **518**(11), 2941 (2010).
- [6] W. Yang, Z. Liu, D. L. Peng, F. Zhang, H. Huang, Y. Xie, Z. Wua, *Appl. Surf. Sci.* **255**(11), 5669 (2009).
- [7] Y. Imanishi, M. Taguchi, K. I. Onisawa, *Thin Solid Films* **518**(11), 2945 (2010).
- [8] J. I. Oda, J. I. Nomoto, T. Miyata, T. Minami, *Thin Solid Films* **518**(11), 2984 (2010).
- [9] S. W. Cho, J. A. Jeong, J. H. Bae, J. M. Moon, K. H. Choi, S. W. Jeong, N. J. Park, J. J. Kim, S. H. Lee, J. W. Kang, M. S. Yi, H. K. Kim, *Thin Solid Films* **516**(21), 7881 (2008).
- [10] K. Sivaramakrishnan, N. D. Theodore, J. F. Moulder, T. L. Alford, *J. Appl. Phys.* **106**(6), 063510 (2009).
- [11] D. Kim, *J. Alloys Compd.* **493**(1-2), 208 (2010).
- [12] J. H. Park, H. K. Kim, H. Lee, H. Lee, S. Yoon, C. D. Kim, *Electrochem. Solid-State Lett.* **13**(5), J53 (2010).
- [13] J. C. C. Fan, F. J. Bachner, *Appl. Opt.* **15**(4), 1012 (1976).
- [14] D. R. Lide, C. R. C. Handbook of Chemistry and Physics, 76th ed., CRC Press, Boca Raton, 1996.
- [15] T. H. Kim, B. H. Choi, J. S. Park, S. M. Lee, Y. S. Lee, L. S. Park, *Mol. Cryst. Liq. Cryst.* **520**(1), 209 (2010).
- [16] H. J. Cho, K. W. Park, J. K. Ahn, N. J. Seong, S. G. Yoon, W. H. Park, S. M. Yoon, D. J. Park, J. Y. Lee, *J. Electrochem. Soc.* **520**, J215 (2009).
- [17] D. R. Sahu, S. Y. Lin, J. L. Huang, *Appl. Surf. Sci.* **253**(11), 4886 (2007).
- [18] H. K. Park, J. A. Jeong, Y. S. Park, S. I. Na, D. Y. Kim, H. K. Kim, *Electrochem. Solid-State Lett.* **12**(8), H309 (2009).
- [19] M. Girtan, *Sol. Energy Mater. Sol. Cells* **100**, 153 (2012).
- [20] P. Kubis, L. Lucera, F. Machui, G. Spyropoulos, J. Cordero, A. Frey, J. Kaschta, M. M. Voigt, G. J. Matt, E. Zeira, C. J. Brabec, *Org. Electron.* **15**(10), 2256 (2014).
- [21] J. A. Jeong, H. K. Kim, *Sol. Energy Mater. Sol. Cells* **93**(10), 1801 (2009).
- [22] M. Fahland, P. Karlsson, C. Charton, *Thin Solid Films* **392**(2), 334 (2001).
- [23] H. K. Park, J. W. Kang, S. I. Na, D. Y. Kim, H. K. Kim, *Sol. Energy Mater. Sol. Cells* **93**(11), 1994 (2009).
- [24] G. Haacke, *J. Appl. Phys.* **47**(9), 4086 (1976).
- [25] M. Kohlstädt, M. Grein, P. Reinecke, T. Kroyer, B. Zimmermann, U. Würfel, *Sol. Energy Mater. Sol. Cells* **117**, 98 (2013).
- [26] H.-H. Liao, L.-M. Chen, Z. Xu, G. Li, Y. Yang, *Appl. Phys. Lett.* **106**, 173303 (2008).

*Corresponding author: chusy@mail.ncku.edu.tw;
tw78787788@yahoo.com.tw